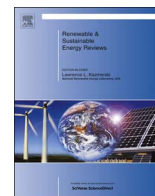




Contents lists available at ScienceDirect

Renewable and Sustainable Energy Reviews

journal homepage: www.elsevier.com/locate/rser

An assessment of Florida's ocean thermal energy conversion (OTEC) resource

James H. VanZwieten*, Lynn T. Rauchenstein¹, Louis Lee

Florida Atlantic University, Southeast National Marine Renewable Energy Center, 777 Glades Road, 33431 Boca Raton, FL, USA

ARTICLE INFO

Keywords:

OTEC
Ocean thermal energy
Thermal energy conversion
Marine renewable energy
Ocean energy
Renewable energy

ABSTRACT

Technological advances in marine renewable energy allow for various methods of extracting energy in the form of electrical power from the ocean. One method is through the process of ocean thermal energy conversion (OTEC). This study assesses the distributions of electrical power that can be extracted from the ocean around the state of Florida. The OTEC resource is analyzed with the combination of a state-of-the-art ocean circulation model, the Hybrid Coordinate Ocean Model, along with a state-of-the-industry OTEC plant model in order to predict the attainable power values offshore Florida. The power predictions are then constrained by local cold deep sea water replenishment to provide an upper limit to the sustainable OTEC resource. The thermal resource is used as input to the plant model to predict the potential power production. The resource data is then validated through the comparison against in situ oceanic measurements to safeguard the quality of the predicted power values.

1. Introduction

Ocean thermal energy conversion (OTEC) is a method of converting solar energy stored as sensible heat in the upper mixed layer of tropical and subtropical oceans into electricity by evaporating an appropriate working fluid in a Rankine cycle operated between warm surface and cold deep water temperatures. The cold deep water used to condense the working fluid originates in the Polar Regions where it sinks towards the sea floor and then travels towards the equator in a cold deep water layer. The resulting thermal stratification is maintained due to the phenomenon that dense, salty water sinks towards the sea floor below the less dense warm water located near the surface. OTEC is commonly considered a viable energy source where thermal gradients exceed approximately 20 °C between surface and deep waters [1]. OTEC technology was first described in 1881 by the French physician, physicist, and inventor, Jacques-Arsene D'Arsonval [2]. D'Arsonval proposed the use of warm surface water from the tropical oceans to vaporize pressurized ammonia through a heat exchanger, then using the vapor to drive a turbine-generator. Cold water pumped from the deep ocean can then be used to re-condense the ammonia vapor. It is noted that relatively large amounts of sea water are required to operate on OTEC plant because of the low efficiencies associated with converting thermodynamic energy to mechanical energy. The upper limit of this efficiency is dictated by the Carnot efficiency, which for 28 °C warm

water and 8 °C cold water is 6.6%. The cycle proposed by D'Arsonval is known as the OTEC closed cycle because the working fluid flows in a closed loop. Closed cycle plants operate according to the Rankine power cycle, analogously to a modern coal or natural gas fired power plant that uses carbon fuel to evaporate water. Like coal and gas plants, OTEC can provide a source of predictable base load power. Other working fluids besides ammonia that have been proposed include propane, various refrigerants, and ammonia-water mixtures [3]. All of these fluids share the common property of a low boiling point within the temperature range of tropical and subtropical ocean surface waters.

The first to attempt to construct a demonstration-scale OTEC plant was led by Georges Claude in 1930. This open cycle plant was installed off the coast of Cuba and produced 22 kW electricity, but no net power [4]. In 1935, Claude designed a 2.2 MW floating plant off the coast of Brazil but was unable to attach the large cold water intake pipe (CWP). Developments in the offshore industry have made deployments of these pipes, which may be as large as 10 m in diameter and 1000 m long, achievable today. Both of Claude's plants were destroyed by weather and waves before net power was produced [5,6].

Investment in OTEC waned in the intervening years before experiencing a surge sparked by the oil embargo of the 1973–4. In 1979, a pilot closed cycle plant called 'Mini-OTEC' was installed atop a barge near the Natural Energy Laboratory of the Hawaiian Authority (NELHA) in Hawaii. The project was led by the U.S. Department of

* Corresponding author.

E-mail addresses: jvanzwi@fau.edu (J.H. VanZwieten), lrauchenstein@gmail.com (L.T. Rauchenstein), llee36@fau.edu (L. Lee).

¹ Present address: Pacific Northwest National Laboratory, PO Box 999, 99352 Richland, WA, USA.

<http://dx.doi.org/10.1016/j.rser.2016.11.043>

Received 16 November 2015; Received in revised form 24 January 2016; Accepted 4 November 2016

Available online xxx

1364-0321/© 2016 Elsevier Ltd. All rights reserved.

Nomenclature

A	cold water pipe cross-sectional area
C_{shb}	cold water pipe static head bias correction
D	cold water pipe diameter
f	friction coefficient of cold water pipe
f_c	quotient of OTEC cold water usage and cold water volumetric flow rate through Florida Straits
g	gravitational constant
h_f	head loss due to pipe friction
L_{fixed}	fixed OTEC power losses
L_{pf}	cold water pipe friction loss
L_{pp}	cold water pump power loss,
L_{sh}	cold water pipe static head loss
L_{ssh}	simplified cold water static head loss
L_{var}	variable OTEC power losses associated with cold water pumping
\dot{m}	cold seawater mass flow rate
N	number of 100 MW OTEC plants
\bar{P}_A	mean annually averaged net power production
P_G	gross PTEC power production
P_G^{LM}	Grose accommodate propriety assumptions made by Lockheed Martin

\bar{P}_{max}	maximum net power for the region using monthly power production averages
P_N	Net OTEC power production
Q	volumetric transport of water through the Florida straits
Q_C	volumetric transport of cold water through the Florida straits
R	radius of Earth
T	Water temperature
T_D	water temperature at the deep water intake depth
T_S	water temperature at the near surface cold water intake depth of 20 m
V	eastward component of the water velocity
z	depth below mean sea surface elevation
ΔT	temperature difference between the warm and cold water resources
ρ	water density calculated as a function of temperature
ρ_D	density of seawater calculated using the cold deep water temperature
ρ_f	constant density value used for calculating head loss
ρ_S	density of seawater calculated using the warm near surface water temperature
η	seawater pump efficiency

Energy (DOE), NELHA, and a consortium of U.S. companies. The plant succeeded in generating > 50 kW gross power (18 kW net) and provided a testing ground for various OTEC design components [7]. A second project, OTEC-1, was installed in 1981 as a testing platform for various heat exchanger and other technologies and was not designed to produce net power [8]. Also in 1981, the Tokyo Electric Power Company and a consortium of Japanese companies constructed a demonstration-scale OTEC plant on the island of Nauru. The plant produced 120 kW gross power (30 kW net) and powered a school and other buildings on Nauru for a few months before being decommissioned [9]. Since then, work has continued in many countries testing heat exchanger and working fluids [10,11]. In 1993, a land-based open cycle plant was designed and installed at NELHA. The plant reached a maximum of 103 kW net power, desalinated water at a rate of 0.4 Ls-1, and operated for six years before being decommissioned [10]. On August 21, 2015, Makai Ocean Engineering launched the first closed-cycle onshore OTEC power plant to be connected to a U.S. electrical grid sited in North Kona, Hawaii at NELHA. The plant is the world's

largest operational OTEC power plant and generates 100 kW of sustainable electricity which is enough to power an estimated 120 Hawaii homes annually [12].

Previous studies have attempted to quantify the magnitude of the global OTEC resource with varying degrees of complexity. Estimates ranging from 5 TW to more than 1000 TW have been quoted. The highest of these values were calculated from total solar energy absorbed by the ocean and the lowest modeling maximum sustainable extractable energy [13–15]. Additional studies have estimated global OTEC potentials using data from the World Ocean Atlas at 1° and later at ¼° horizontal resolution [1,15]. These analyses represent a valuable source of OTEC information, but data are limited to the waters in which depth exceeds 1000 m, lacking information for many coastal and island regions where water is shallower. Rajagopalan and Nihous later inserted mass flow singularities into an ocean general circulation model (OGCM) to simulate the redistribution of water [15,16]. The latter study predicted an absolute power limit at 30 TW, beyond which increasing water flow rates would induce mixing of the thermocline and

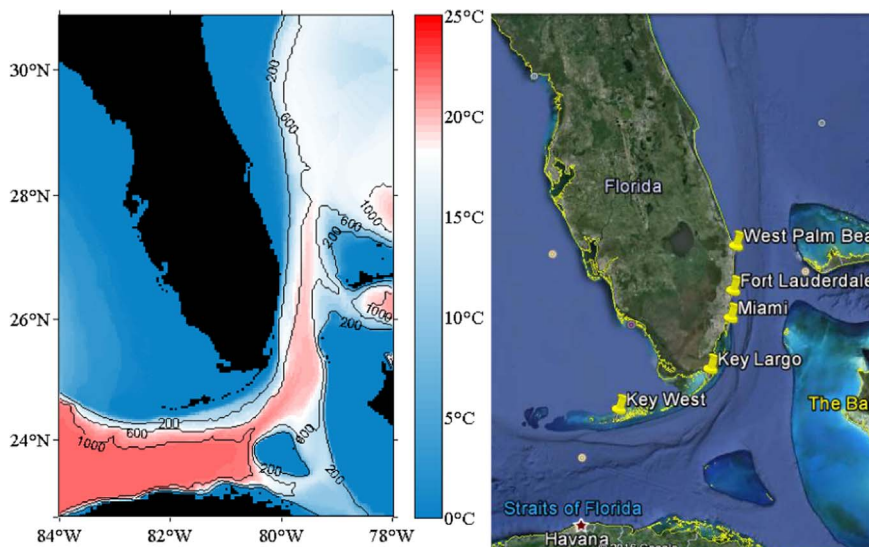


Fig. 1. Annual mean ΔT between 20 m and the shallower of 1000 m or the ocean floor for Florida.

reduce the global power potential [16]. Further studies include mapping the thermal difference between proposed cold and warm water resource depths and mapping the predicted power output from representative OTEC plant model [17].

Because Florida's waters are shallower than 1000 m, previous global OTEC assessments have not provided data for in the region. Leland et.al. [18] calculated the temperature difference off South Florida's Atlantic coast using CTD measurements taken between 20 m beneath the surface and about 10 m above the ocean floor. The study found annually average values along transects extending from Miami, Fort Lauderdale, Boynton, and Stuart, FL, as high as 21.7, 21.6, 21.1, and 20.6 °C, respectively, with 5–6 °C temperature swing between mean summer and winter values. Using an OTEC plant model it was estimated these thermal values would correspond to power output about 110–125% the design power for a 100 MW plant [18]. Temperatures measured atop the Miami Terrace, a large underwater plateau offshore Miami and Fort Lauderdale, revealed annually averaged temperature difference values as high as 20 °C in waters as shallow as 165 m, making the Miami Terrace a site of special interest [19].

In this paper the ocean thermal energy resource is estimated using the HYbrid Coordinate Ocean Model with Navy Coupled Ocean Data Assimilation (HYCOM+NCODA; for short in this document, 'HYCOM'). HYCOM was created as part of a multi-institutional effort led by Florida State University, the Rosenstiel School at the University of Miami, the Naval Research Laboratory/Stennis Space Center, and the National Oceanographic and Atmospheric Administration [20]. Model calculated temperature data are used to estimate electrical power generated by an OTEC plant. The HYCOM model is a well-documented [21,22] community model of global ocean dynamics and thermodynamics, which incorporates a hybridized vertical coordinate which transitions from isopycnal in stratified waters to terrain-following (sigma) in shallow coastal regions, and to z-level in mixed layer unstratified seas. The model generates a forecast, which is then adjusted toward physical measurements by assimilation of available satellite altimeter data along with in situ sea surface temperature and vertical temperature and salinity profiles acquired from XBTs, ARGO floats, and moored buoys. Surface forcing includes wind stress, wind speed, heat flux (using bulk formula), and precipitation. Data were acquired from the HYCOM Gulf of Mexico experiment 31 (exp31) [20]. Temperature arrays spanning Florida and its waters from 22°46.8' to 30°48.0'N, 78°00.0'–84°00.0'W, including the water depths down to 1000 m, were analyzed. These data are available as hourly snapshots, and in this study the daily snapshots from hour 00Z are used for computing all long-term averages. Data from 00Z are hereafter referred to as 'daily' data. Horizontal resolutions for these data are 1/25° latitude and longitude, corresponding to ~4 km resolution at the latitudes considered. Depth resolution in the area varies from 5 m near the ocean surface to 100 m at depths below 300 m.

The purpose of this paper is to provide an assessment of the OTEC electricity production potential off Florida, both in terms power production per OTEC device and overall OTEC power production capacity within the Florida Straits. Numerical models were used to map the thermal characteristics and OTEC potential statewide, as well as the volumetric flow rates through the Florida Straits. Thermal and flow measurements are then used to validate these predictions. Florida's offshore thermal distribution is presented in Section 2. An OTEC plant model and electrical power production predictions for offshore Florida are presented in Section 3, along with the relationship between power production and the cold water utilized to produce this power in the Florida Straits. Comparison between HYCOM data to in situ data are presented in Section 4, and final conclusions are drawn in Section 5.

2. Florida's thermal resource

This section evaluates the offshore thermal structure of Florida, as this is directly related to the OTEC power that can be produced. Generally, with every 1 °C increase in difference between the utilized warm and cold water resources, the extractable power increases by about 15% [1]. Therefore, the power resource for OTEC can be visualized without dependence on plant type by depicting the temperature differential as a proxy.

To compute the temperature difference between the warm and cold water resources, ΔT , both shallow water and cold deep water are utilized. Shallow water temperature, T_s , is defined at the assumed depth of the shallow water intake pipe of 20 m, and deep water temperature, T_D , is assumed to be derived from the deepest point in the vertical depth stratification to a maximum depth of 1000 m. This depth limit was imposed in consideration of the difficulties expressed by the industry of deploying such a long intake pipe. The mean annual temperature was calculated using daily snapshot temperatures of the HYCOM model taken at 00Z and spanning April 1, 2009–March 31, 2012 (Fig. 1).

The value and location of the maximum temporally averaged ΔT for HYCOM depth levels between 200 and 1000 m are presented in Table 1. Under the assumption where appreciable values of net power begin to occur in waters where $\Delta T = 18$ °C, none of the waters shallower than 200 m are suitable for OTEC power generation. High values of ΔT exist nearest to shore off the coasts of West Palm Beach, Fort Lauderdale, Miami, Key Largo, and Key West. Maximum ΔT values for shorter pipe lengths (200–400 m) occur offshore the Miami area. However, for longer pipe lengths, maximum ΔT moves successively south to the waters below Key West. The maximum temperature differential for the annually averaged period was 22.41 °C and was located approximately to the south of Key West.

3. Power production potential

This section discusses the representative OTEC plant utilized to quantify power production. Mean annual power production estimates for offshore Florida are then presented, followed by the predicted variability of produced power. Finally, total power production potential between Key West and Cuba is compared with the percentage of the cold water resource necessary to generate this electrical power.

3.1. OTEC plant model

This sub-section provides an overview of the OTEC plant model utilized in this study, which is presented in greater detail by [3,17]. This model calculates the net power production of a single OTEC plant as a function of water temperatures and cold water pipe length. It was created to represent the 100 MW net power/150 MW gross power closed cycle plant that Lockheed Martin/Makai Ocean Engineering designed as part of a contract with the U.S. Naval Facilities Engineering

Table 1
Maximum annual ΔT and its location for every depth level around Florida.

Depth (m)	Distance from US shore (km)	ΔT_{max} (°C)	Location
200	12	17.59	25°39.4'N, 80°02.4'W
250	12	18.73	25°52.4'N, 80°00.0'W
300	19	19.40	25°37.2'N, 79°57.6'W
400	25	20.12	25°32.9'N, 79°55.2'W
500	46	20.60	24°47.3'N, 80°07.2'W
600	51	21.14	24°42.9'N, 80°07.2'W
700	60	21.37	24°36.4'N, 80°07.2'W
800	63	21.71	24°08.0'N, 81°00.0'W
900	71	22.05	24°03.6'N, 81°07.2'W
1000	98	22.41	23°41.6'N, 82°04.8'W

Table 2
Assumptions for the 100 MW net/150 MW gross power OTEC plant model.

Warm water mass flow rate	460,000 kg/s
Cold water mass flow rate (\dot{m})	366,000 kg/s
Ammonia mass flow rate	4060 kg/s
Turbine expander efficiency	86%
Ammonia pump efficiency	75%
Seawater pump efficiency (η)	80%
Generator efficiency	97.5%
Evaporator UA	1410 MW/°C
Condenser UA	1350 MW/°C
Head loss due to friction (h_f)	0.0008356z
Gravitational constant (g)	9.81 m/s ²
Friction factor (f)	0.007933
Pipe diameter (D)	10 m
Pipe intake area (A)	78.5 m ²
Head loss water density (ρ_f)	1025 kg/m ³
Water density (ρ)	(-0.00599T ² +0.031T+1025) kg/m ³

Command (NAVFAC) for a location off Kahe Point, Hawaii [23]. The model represents a single-stage, closed cycle OTEC plant, using anhydrous ammonia as the working fluid.

For this plant model, the OTEC net power production (P_N) is calculated using three components: gross power (P_G), based on the governing thermodynamic equations of a Rankine cycle; variable losses (L_{var}), associated with cold water pumping; and fixed losses (L_{fixed}), associated with all other pumping and transmission within the plant,

$$P_N(MW) = P_G - L_{fixed} - L_{var}. \quad (1)$$

The gross power production equation combines Carnot efficiency, Carnot to Rankine efficiency, and heat balance across the evaporator. The formula for P_G is modified from an equation given by Nihous (2007) [15] to accommodate propriety assumptions made by Lockheed Martin [3] (P_G^{LM}), and then simplified to a linear equation [17]:

$$P_G^{LM}(MW) = \frac{106.22 * \Delta T^2}{T_s - 0.25 * \Delta T + 273.15} \approx P_G(MW) = 13.89 \Delta T - 149.71, \quad (2)$$

where temperatures are given in °C. The linear and non-linear equations were compared using data from 28 HYCOM locations selected to represent the full array of ocean conditions [3]. The linearized formula was found to fit the original formula with an R² value of 0.99979 [3]. Therefore, the linear equation is used in all presented power calculations.

The value of L_{fixed} is based on the particular assumptions of the plant model listed in Table 2. Using these plant properties the losses due to the cold water intake, condenser and distribution pumping, evaporator and distributing pumping, and ammonia pumping were calculated. The derivations of each of these components were presented

in [17] resulting in a total fixed loss of:

$$L_{fixed}(MW) = 42.7. \quad (3)$$

Variable losses, L_{var} , represent the sum of pipe friction loss, L_{pf} , and static head loss, L_{sh} :

$$L_{var}(MW) = L_{pf} + L_{sh}. \quad (4)$$

Pipe friction loss is calculated based on pipe smoothness, pipe diameter, and water velocity. Static head loss is calculated as a product of pump power loss, static head bias correction, and simplified static head loss.

Pipe friction loss and static head loss are respectively calculated as:

$$L_{pf} = \frac{h_f \dot{m} g}{\eta} = \frac{f \left(\frac{\dot{m}}{\rho_f A} \right)^2 \dot{m} g}{2 D g \eta} = 0.0038z, \quad (5)$$

and

$$L_{sh} = (L_{pp} + L_{ssh} + C_{shb})z, \quad (6)$$

where L_{pp} is the pump power loss, L_{ssh} is the simplified static head loss, and C_{shb} static head bias correction. These are respectively calculated from:

$$L_{pp} = \frac{\dot{m} g z}{\eta} = 4.488z, \quad (7)$$

$$L_{ssh} = \frac{\rho_D - \rho_S}{\rho_D} = \left(\frac{-0.00599T_s^2 + 0.031T_s + 1025}{-0.00599(T_s - \Delta T)^2 + 0.031(T_s - \Delta T) + 1025} - 1 \right), \quad (8)$$

$$C_{shb} = 5.234(10^{-10})z^3 - 1.378(10^{-6})z^2 + 1.313(10^{-3})z - 0.6541. \quad (9)$$

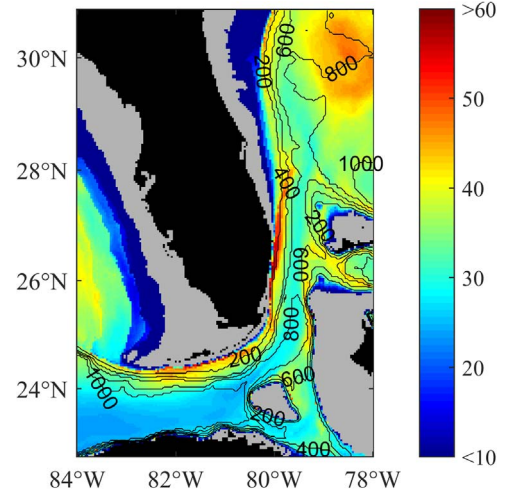


Fig. 3. Standard deviation of OTEC power production in MW.

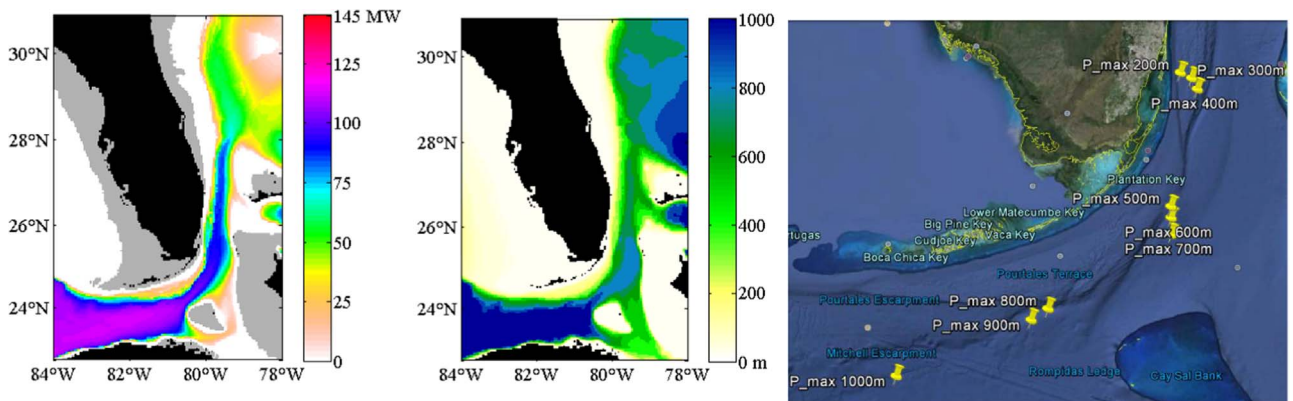


Fig. 2. Power (left) and cold water depth (middle), and locations of maximum calculated OTEC power for depths from 200 to 1000 m (right) around Florida.

Table 3
Maximum time averaged power and its location for discrete depth levels around Florida.

Depth (m)	Distance from US shoreline (km)	P_{max} (MW)	Location of P_{max}
200	12	50.2	25°39.4'N, 80°02.4' W
300	19	74.6	25°37.2'N, 79°57.6' W
400	25	83.8	25°32.9'N, 79°55.2' W
500	46	90.0	24°47.3'N, 80°07.2' W
600	51	96.8	24°42.9'N, 80°07.2' W
700	60	99.4	24°36.4'N, 80°07.2' W
800	63	103.6	24°07.9'N, 81°00.0' W
900	71	107.7	24°03.6'N, 81°07.2' W
1000	98	112.2	23°41.6'N, 82°04.8' W

To create power predictions, these equations are utilized at every grid point in the temperature matrix for each daily HYCOM file beginning April 1, 2009 and continuing for three years. The mean net electrical power production averaged over the three year period, \bar{P}_A , was evaluated at each lat/lon location for all evaluated depths (up to 1000 m) to locate the depth of cold water at each lat/lon location yielding maximum power. These depths were utilized for the power production maps (Figs. 2 and 3).

3.2. Mean annual power

This sub-section presents the calculated three year temporally averaged net electrical power production statewide for the representative 100 MW OTEC plant. Net average electrical power production exceeding 100 MW is calculated to be achievable off the southern coast of Florida (Fig. 3). The thermal resource allowing for net positive power production is located tens of kilometers offshore from the east coast and hundreds of kilometers from the west coast of Florida. This OTEC resource hugs the shore closely in the waters stretching from Miami to West Palm Beach, where the continental shelf is shallowest. The shortest distance from the shoreline to a point where net power can be produced by OTEC is about 8 km, between the HYCOM point with center 25°56.7'N, 80°02.4'W and the Florida coast at Sunny Isles near North Miami. At 26°09.6'N, 80°00.0'W, near Lauderdale Lakes, power is producible ~9–10 km from shore.

It is possible to generate $\bar{P}_A > 80$ MW within 44 km south off the shore of Key West (24°08.0'N, 81°55.2'W) using a cold water pipe reaching 700 m deep. $\bar{P}_A > 100$ MW is possible within 56 km of shore using a cold water pipe reaching 900 m deep (24°01.4'N, 81°55.2'W). The nearest point at which $\bar{P}_A > 80$ MW is possible east of the Florida mainland with its center at (25°50.2'N, 79°50.4'W), 27 km east of Miami. A cold water pipe in this location would need to reach to a 400 m depth. $\bar{P}_A > 100$ MW is not possible to the east of the Florida mainland.

Bathymetry and net power potential decreases eastward and northward through the Florida Straits, lifting from 1000 m at the inlet to 700 m at its deepest point offshore West Palm Beach. However, net average power can still be generated in as little as 125 m deep water in the Straits. The value and location of maximum \bar{P}_A achievable at each cold water depth level are presented in Table 3, with the location also provided in Fig. 2(Right).

The table shows that an OTEC plant utilizing a long Cold Water Pipe (CWP) with a length of 1000 m would generate the greatest amount of power if sited south from the Florida Keys. An OTEC plant

utilizing a short to medium-length CWP (< 500 m) would produce the most power if sited offshore from Miami/Fort Lauderdale. An OTEC plant with a 300 m CWP is projected to generate a maximum \bar{P}_A of 74.6 MW in the shallow-water location off the east coast of the Florida mainland, and only 62.6 MW near the Keys. A plant using a 400 m pipe is projected to generate 84 MW off the east coast of the Florida mainland and only 77.5 MW in the Keys.

3.3. Seasonal power

The seasonal variation of net power output on the shallow water temperature and total site depth is pronounced. The average monthly maximum power for the evaluated region, \bar{P}_{max} , is listed in Table 4 below. The locations of \bar{P}_{max} varied month by month, but were consistently situated to the south of the Florida Keys within the 1000 m cold water isobaths.

The seasonally-averaged values of \bar{P}_{max} for summer, fall, winter, and spring are 141.5, 129.6, 86.2, and 97.5 MW, respectively. The point of seasonal maximum power is found uniformly in the southwestern corner of the map (Fig. 2 – Left), within the 1000 m cold water isobath. Values are highest in summer and lowest in winter, and higher in the fall than in the spring. These seasonal fluctuations of power match the energy demand in Florida, with the highest OTEC power production potential occurring in the summer months when power consumption is greatest due to the use of air conditioning. South of the Florida Keys power values increase from east to west. During the winter, the OTEC resource pushes tens of kilometers offshore both to the south of the keys and to the east of South Florida. Above 28°N, the resource becomes negligible in the winter months.

Fig. 3 depicts the standard deviation of OTEC power, which is highest in shallower water locations along the boundary of the continental shelf south of the keys and east of Florida, as well as north of the Bahamas atop the Blake Plateau (~29–31°N). The Blake Plateau is located along the northeastern section of the map in about 700–800 m deep water, where power is low (< 60 MW) for all seasons and where net power cannot be generated in winter. The area of least power deviation, $\sigma = 22$ MW, is located in deep water just north of Cuba, at 23°24.05'N, 80°45.6'W.

3.4. Total power in the Florida straits

OTEC implementation in this region is limited by the rate of replenishment of deep, cold water [8]. Therefore, an estimate of cold water flow through the Straits can help to gauge the number of plants that can be operated in the region. The Florida Current represents 20% of the mass flow of the Gulf Stream, with an annual mean transport estimated at 32.1 ± 3.3 Sverdrups (Sv) [24]. Previous studies have suggested around 0.5 Sv of water below 7 °C [24] and 3.9 Sv of water below 12 °C [25] flow through the Florida Current at 27°N. For this study, cold water is defined as water ≤ 9 °C, which is chosen because it

Table 4
Location of maximum power for every month (Florida).

Month (Season)	\bar{P}_{max} (MW)	Location
January (Winter)	83.6	23°26.2'N, 83°45.6'W
February (Winter)	79.8	23°39.4'N, 82°02.4'W
March (Spring)	84.8	23°10.8'N, 83°33.6'W
April (Spring)	95.6	23°26.2'N, 82°52.8'W
May (Spring)	114.0	23°37.2'N, 82°04.8'W
June (Summer)	136.2	23°48.2'N, 81°33.6'W
July (Summer)	140.2	24°25.5'N, 83°55.2'W
August (Summer)	152.3	24°29.8'N, 83°57.6'W
September (Fall)	145.3	24°27.6'N, 83°52.8'W
October (Fall)	130.4	24°25.5'N, 83°52.8'W
November (Fall)	113.7	24°23.2'N, 83°57.6'W
December (Winter)	98.0	23°24.0'N, 84°00.0'W



Fig. 4. Location of Transect 'A' spanning from near La Habana, Cuba at (23.175°N, 82.12°W) to near the Dry Tortugas National Park, United States (24.6°N, 82.12°W).

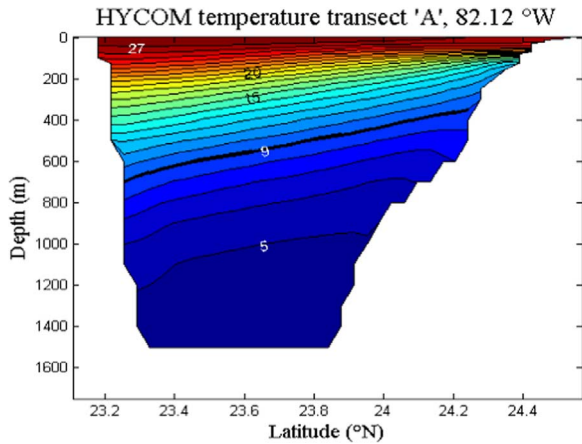


Fig. 5. Transect at location "A" showing cold water temperature at the entrance to the Florida straits.

approximates the warmest deep water temperature capable of being used to produce at least 80% design net power for an OTEC plant in the region. This value is also close to the mean cold water temperature for all the global OTEC-valid points of 9.96 °C [3].

Daily temperature and current velocity values were acquired from HYCOM exp31 across a transect 'A', spanning approximately 158 km, drawn at the entrance to the Florida Straits (Fig. 4) for dates spanning April 1, 2009–March 31, 2012. Only the velocity vector component perpendicular to this transect is needed in order to calculate transport, i.e., the eastward velocity component, V . HYCOM gridding at this transect is resolved latitudinally into about $1/25^\circ$ (~ 4 km) increments and along the ocean depth dimension in increments (Δz) ranging from 5 m at the surface to 100 m at depths below 300 m. The three-year mean temperature at 'A' is shown in Fig. 5.

The temperature and velocity transects were averaged into monthly and full dataset means. These mean values were used to determine the total transport through all grid cells with temperatures ≤ 9 °C. The transport of water, Q , through any singular transect grid cell is

$$Q \left(\frac{m^3}{s} \right) = V \cdot \Delta z \cdot \left(\Delta Lat \cdot \frac{\pi R}{180} \right), \quad (10)$$

Table 5

Temperatures along the eastern land-ocean interface for Florida current transect at 27° N.

Temperature at east intersect (°C)					
	Date range	200 m	400 m	600 m	750 m
CTD	1982–2007	13–14	9–10	7–8	6–7
PEGASUS	1982–1984	11–12	8–9	7–8	6–7
HYCOM	2009–2012	12–13	8–9	6–7	6–7

with Earth's radius, R , is set equal to 6371 km. Then the total transport of cold water, Q_C , is

$$Q_C = \sum Q_{T \leq 9^\circ C}. \quad (11)$$

The total mean transport for the full dataset was calculated by this method to be 36.6 Sv, slightly above the upper bound of the 32.1 ± 3.3 Sv estimate given by [24]. This may indicate a slight upward bias to current velocities in the model. The total mean Q_C was calculated to be 3.9 Sv. If each plant consumes cold water at a volumetric rate of $F_c = 357 \text{ m}^3/\text{s}$, the number of plants, N , which can be sustained by a fraction, f_c , of Q_C is given by

$$N = \frac{f_c \cdot Q_C}{F_c}. \quad (12)$$

Determination of a maximum f_c that is appropriate for limiting environmental impacts is outside the scope of this study, though these environmental impacts have been studied by others [26,27]. However, the Straits could support 10,924 of the Lockheed Martin 100 MW plants, assuming that 100% of the incoming cold water is consumed. Alternately, a single 100 MW OTEC plant would require 0.01% of the incoming cold water, and 1% of the incoming water could support about 109 plants. This calculation does not account for the impact that artificial mixing of warm and cold water will have on downstream OTEC plants, which will become increasingly important as the number of OTEC plants increases. Since a nominal 100 MW plant installed in this region can produce an average net power of 110 MW, utilizing 0.01% of Q_C could net 110 MW and 1% of Q_C could net 12 GW of electrical power, which is equivalent to 2.6% of the total 2011 U.S. power production (2011 total US electrical energy production was estimated at 4100 TWh by [28], or on average 461 GW).

4. HYCOM comparisons with in situ data

4.1. Thermal comparisons

In order to evaluate the accuracy of HYCOM exp31-predicted temperature and current velocity values, they are compared with historic measurement based averages and contemporary measurements collected on overlapping dates. These recent measurements include vessel-deployed Current/Temperature/Depth sensors (CTDs) and bottom-mounted Acoustic Doppler Current Profilers (ADCPs).

Historic averages were used from Xu et al. [25] where 154 CTD casts were used to estimate a multi-decadal mean temperature of the 27°N transect across the Florida Current, spanning 1982–2007. In a second study, Leaman et al. [29] estimated temperature across the same transect using PEGASUS acoustic current profilers spanning 1982–1984 (857 profiles). Results of both studies were compared with the three-year mean HYCOM temperature spanning April 2009–March 2012 at 27°N by [3]. Because this research is focused on evaluating the OTEC resource for Florida, transect temperatures are compared along the land-ocean interface on the western half of the basin. HYCOM temperatures at $z \geq 200$ m all fall within a range comparable to those of CTD and PEGASUS for the same depths (Table 5).

The utilized HYCOM exp31 dates temporally overlap CTD transects

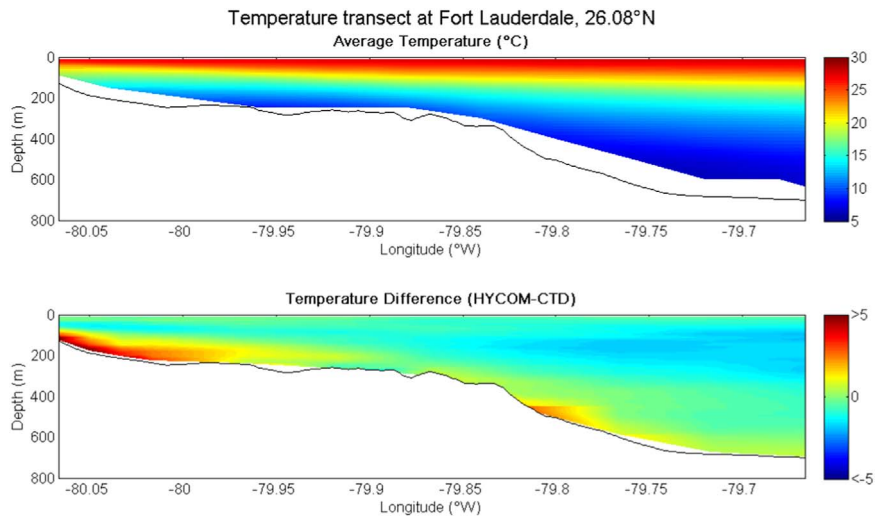


Fig. 6. Average HYCOM predicted temperature profile (Top), and temperature difference (HYCOM-CTD) between HYCOM predictions and CTD measurements (Bottom) off Fort Lauderdale. Calculations based on 29 CTD transects dates.

conducted off SE Florida and a basic statistical comparison is presented here, with a more comprehensive comparison provided in [3]. The CTD temperature measurements were collected as described by Leland [18]. A total of 51 CTD cast transects (9–11 casts per transect) were collected between April 2009 and February 2011, in water depths ranging from around 100 m near shore to 800 m at the eastern end of the transect. Four transects were defined along lines of constant latitude extending from Florida's Atlantic coast at Stuart (27.18°N, 6 cast dates), Boynton Beach (26.63°N, 6 cast dates), Fort Lauderdale (26.08°N, 29 cast dates), and Miami (25.51°N, 10 cast dates) through the extent of the EEZ. For every day on which CTD data were collected, HYCOM temperature predictions from grid points surrounding the CTD data were interpolated linearly to the CTD transect latitude. These HYCOM temperatures were then interpolated with depth using cubic spline interpolation to obtain the same 1 m depth resolution as the CTD record. The coldest mean bottom water temperatures for a given location measured by CTD for each cast transect line from north to south, respectively, are 6.6, 6.2, 5.8, and 5.9 °C. The HYCOM generated temperature transect at Fort Lauderdale is compared with CTD cast data in Fig. 6. These results show that the near bottom and near surface HYCOM estimates are typically within 1 °C of the CTD measurements at this latitude, with the exception being that HYCOM significantly over-predicts the near bottom temperature (under-predicting the OTEC resource) near shore in water depths between 150 and 250 m.

Here, the mean ΔT was under-predicted by more than 2 °C, suggesting that the HYCOM predicted power output for this shallow water area was also significantly under-predicted.

At the cast locations, HYCOM predicted near surface temperatures (20 m depth) with minimal error (mean errors less than 0.5 °C) at all cast sites (Fort Lauderdale shown in Fig. 7), with error defined as the difference between HYCOM estimates and CTD measurements. These near surface predictions typically became more accurate moving eastward along the transect line, with the mean error progressing from north to south, at -0.11 , -0.30 , -0.23 , and 0.07 °C. At the deepest location where both HYCOM and CTD data are available, temperature error decreases as the measurements progress eastward (Fort Lauderdale shown in Fig. 7). However, while HYCOM exhibits a consistent trend of minimally under-predicting water temperatures at 20 m, near bottom mean HYCOM temperature errors are scattered both above and below zero. The near shore HYCOM calculated near bottom temperatures in Fort Lauderdale were over-predicted by approximately 1.5–2 °C. This would mean that the HYCOM calculated mean ΔT of approximately 18 °C near 26°04.8'N, 80°03.0'W should actually be closer to an estimate of 19.5–20 °C. This would likely increase the HYCOM calculated mean OTEC power production by approximately 21–28 MW in this area.

The easternmost values for near bottom HYCOM temperature error for each transect were 0.13, -0.55 , -0.13 , and 0.15 °C from north to

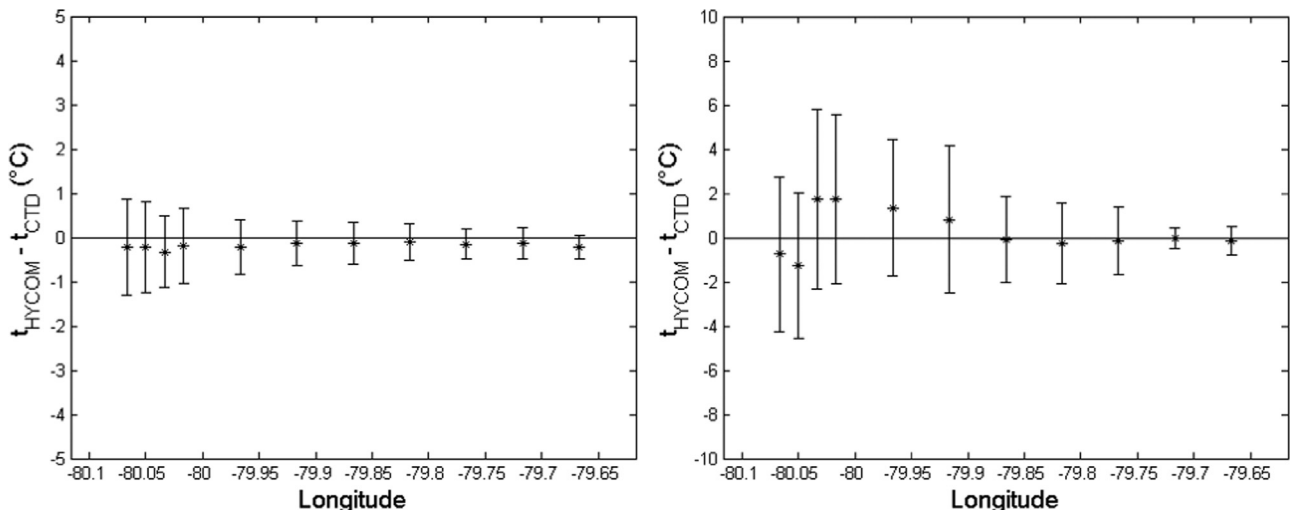


Fig. 7. HYCOM-CTD temperature difference near the sea surface, $z=20$ m, (Left) and near the seafloor (Right) for the CTD transect performed off Fort Lauderdale.

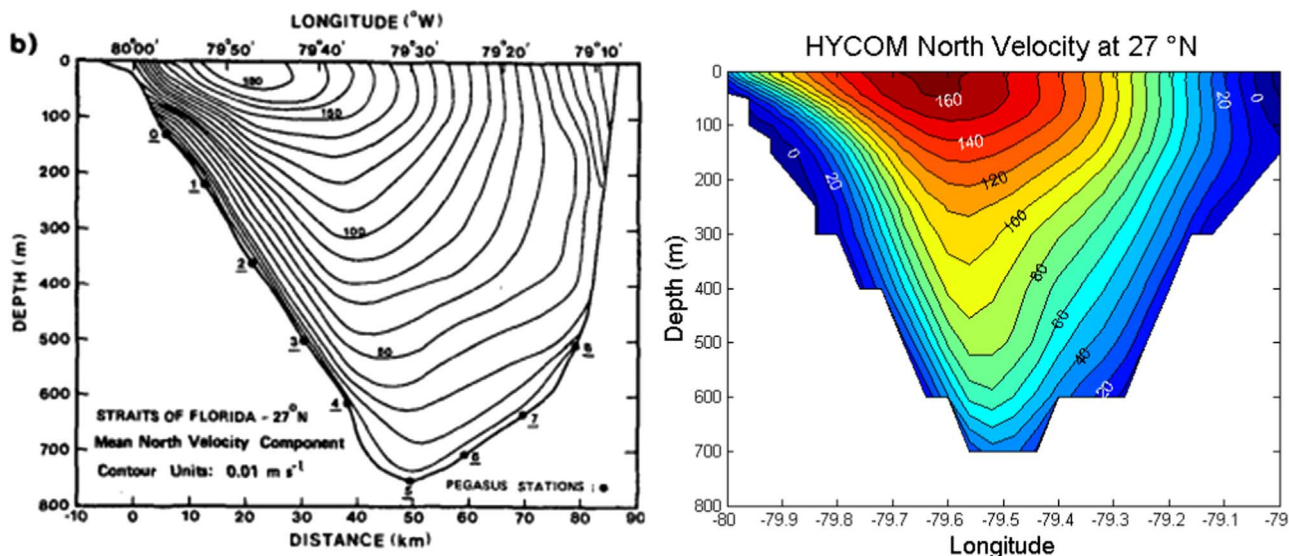


Fig. 8. Historical and HYCOM north velocity transect, 27°N (Left figure reproduced from Leaman et al., [29]).

south, respectively. The combined temperature differences of the modeled vs. measured shallow and deep water would lead to modest power differences at the eastern most cast locations of -3.3 , 3.5 , -1.4 and -1.1 MW, respectively. These temperature measurements fall in a practical range of values for useful power generation with an under-prediction of HYCOM's estimates leading to significantly greater potential OTEC power production.

4.2. Current comparisons

To help assess the accuracy of HYCOM at predicting the cold water transport through the Florida Straits, the 3-year mean northward current velocity at 27°N from HYCOM exp31 spanning April 1, 2009–March 31, 2011 is compared against a transect produced by Leaman, et al. [29] at the same latitude using data from 1160 PEGASUS acoustic profiles taken over two years from 1982 to 1984 (Fig. 8). HYCOM predicted a slightly slower temporally averaged northward maximum sea surface velocity and higher values near the sea floor. As an example, maximum temporally averaged north water velocities at depths of 200, 400, and 600 m calculated from PEGASUS data are 120, 80, and 35 cm s^{-1} , respectively. The corresponding maxima from HYCOM are 120, 95, and 65 cm s^{-1} , with the deepest values nearly double that recorded by PEGASUS.

The volume transport of the Florida Current across the 27°N transect has been studied since 1880 [24,30–33]. Meinen et al. [34] used over 300 shipboard sections and more than 25 years of daily cable observations to estimate transport of the Florida Current across 27°N at 32.1 ± 3.3 Sv. The HYCOM-derived transport calculated at 34.3 Sv [3] suggests that HYCOM provides a good estimate of the overall volumetric transport through the Florida Straits.

The volumetric transport of cold water ($T \leq 9^\circ\text{C}$) is of particular interest for OTEC applications as this quantity imposes an upper limit to the number and spacing of plants in a region. Therefore, the HYCOM calculated cold water transport is compared to measurement based cold water volumetric transport estimates. Leaman et al. [29] estimated that 3.9 Sv of water with a temperature between 7 and 12 °C would be transported northward through the Florida Current at 27°N. Hall and Bryden [24] estimated the Florida Current flow at 5.0 Sv for water at 7–12 °C and 0.5 Sv flow of water $< 7^\circ\text{C}$ at a location of 26°N. The average volumetric flow rate of cold water ($T \leq 9^\circ\text{C}$) calculated using HYCOM data near the entrance of the Florida Straits at 82.12°W, represented by Line A in Fig. 4, is 3.9 Sv. At the 27°N transect HYCOM calculated cold water ($T \leq 9^\circ\text{C}$) volumetric flow rate is slightly less at

3.7 Sv. Both HYCOM estimates fall within a reasonable range of the measurement based cold water volumetric flow rates, suggesting the HYCOM based volumetric flow rate estimates utilized in Section 3.4 are appropriate.

5. Conclusions

Ocean thermal data generated by the HYCOM ver31 was used to estimate the power that can be produced by a nominal 100 MW (net), single stage, closed cycle OTEC plant sited off the Florida's coastline. Three year averaged power production estimates predicted that south of the Florida Keys and east of the Florida mainland 112 MW and 90 MW of net power can be produced. This resource is seasonally dependent with a maximum net power production potential of 152 MW in August and minimum of 78 MW in February, matching the seasonal trends of power demand in the region. Between Key West and Cuba a single OTEC plant is calculated to consume approximately 0.01% of the cold water volumetric flow rate. HYCOM comparisons with measured thermal and water velocity data show that it is an appropriate model for estimating the OTEC potential in this region, with the greatest error in shallow water regions.

Acknowledgements

Funding for this work was provided by the U.S. Department of Energy's Wind and Water Power Program under award DE-EE000264 to Lockheed Martin Corporation, and directly by the Lockheed Martin Corporation. SNMREC is supported by the U.S. Department of Energy and the State of Florida.

References

- [1] Nihous GC. Mapping available ocean thermal energy conversion resources around the main Hawaiian islands with state-of-the-art tools. *J Renew Sustain Energy* 2010;2(4):043101.
- [2] d'Arsonval A. Utilisation des forces naturelles. *Avenir de l'électricité. Rev Sci Tech* 1881;17:370–2.
- [3] Rauchenstein LT. Global distribution of ocean thermal energy conversion (OTEC) resources and applicability in U.S. Waters near Florida [thesis]. Boca Raton (FL): Florida Atlantic University; 2012.
- [4] Claude G. Power from the tropical seas. *Mech Eng* 1930;52(12):1039–44.
- [5] Takahashi M. "Umi ninemuru shigen ga chikyuu osukuu" Tokyo, Japan: Asunarysobo, 1991, (transl.: K. Kitazawa, P. Snowden, Deep ocean water as our next natural resource. Tokyo: Terra Scientific Publishing Co.; 2000, ch. 2, pp. 10–22).
- [6] Chiles JR. The other renewable energy. *Invent Tech Winter* 2009;23(4):24–35.
- [7] Owens WL, Trimble LC. Mini-OTEC operational results. *J Sol Energy Eng*

- 1981;103(3):233–40.
- [8] Lorenz JJ, Yung D, Howard PA, Panchal CB, Powcher FW. OTEC-1 Power system test program: performance of one-megawatt heat exchangers. Argon Natl Lab 1981, Report no: ANL/OTEC-PS-10.
- [9] Mitsui T, Ito F, Seya Y, Nakamoto Y. Outline of the 100 kW OTEC pilot plant in the Republic of Nauru. *IEEE Trans Power Appar Syst* 1983(9).
- [10] Vega LA. Ocean thermal energy conversion primer. *Mar Tech Soc J Winter* 2003;6(4):25–35.
- [11] Fujita R, Markham AC, Diaz JE, Garcia JRM, Scarborough C, Greenfield P, et al. Revisiting ocean thermal energy conversion. *Mar Policy* 2012;36(2):463–5.
- [12] Makai Ocean Engineering [Internet]. Kailua (HI), USA: Makai connects world's largest ocean thermal plant to U.S. grid Available from: (http://www.makai.com/makai-news/2015_08_29_makai_connects_otec/) [updated 2015 August; cited 2016 January 21].
- [13] Zener C. Solar sea power. *Phys Today* 1973;26:48–53.
- [14] Zener C. The OTEC answer to OPEC: solar sea power. *Mech Eng* 1977;99(12):26–9.
- [15] Nihous GC. A preliminary assessment of ocean thermal energy conversion resources. *J Energy Resour* 2007;129:10–7.
- [16] Rajagopalalan K, Nihous GC. Estimates of global ocean thermal energy conversion (OTEC) resources using a general ocean circulation model. *Renew Energy* 2013;50:532–40.
- [17] Ascari M, Hanson HP, Rauchenstein L, VanZwieten J, Bharathan D, Heimiller D, et al. Ocean thermal extractable energy visualization. Final Report. U.S. Department of Energy; 2012 March 30.
- [18] Leland AE, Driscoll FR, VanZwieten JH, Nagurny NJ, Howard RJ. Ocean thermal energy capacity estimation and resource assessment of Southeast Florida, In: Proceedings of the offshore technology conference, Houston, Texas; 2010 May 3–6, no. OTC-20559-PP.
- [19] Leland AE. A resource assessment of southeast florida as related to ocean thermal energy [thesis]. Boca Raton (FL): Florida Atlantic University; 2009.
- [20] Consortium for data assimilative modeling [Internet]. HYCOM Overview. Available from: (www.hycom.org) [cited 2016 January 22].
- [21] Chassignet EP, Hurlburt HE, Smedstad OM, Halliwell GR, Hogan PJ, Wallcraft AL, et al. The HYCOM (hybrid coordinate ocean model) data assimilative system. *J Mar Syst* 2007;65:60–83.
- [22] Chassignet EP, Hurlburt HE, Metzger EJ, Smedstad OM, Cummings JA, Halliwell GR, et al. US GODAE: global ocean prediction with the hybrid coordinate ocean model (HYCOM). *Oceanography* 2009;22:64–75.
- [23] Nagurny J, Martel L, Jansen E, Plumb A, Gray-Hann P, Heimiller D, et al. Modeling global ocean thermal energy resources, In: Proceedings of the IEEE oceans conference, Kona, Hawaii; 2011 September 19–22, no. 110422-145.
- [24] Hall MM, Bryden HL. Direct estimate and mechanisms of ocean heat transport. *Deep Sea Res Part A* 1982;29(3):339–59.
- [25] Xu X, Schmitz WJ, Hurlburt HE, Hogan PJ. Mean Atlantic meridional overturning circulation across 26.5°N from eddy-resolving simulations compared to observations. *J Geophysical Res: Oceans* 2012;117(C3).
- [26] Jia Y, Nihous GC, Richards KJ. Effects of ocean thermal energy conversion systems on near and far field seawater properties – a case study for Hawaii. *J Renew Sustain Energy* 2012;4(6), no 063104.
- [27] Grandelli P, Rocheleau G, Hamrick J, Church M, and Powell B. Modeling the physical and biochemical influence of ocean thermal energy conversion plant discharges into their adjacent waters. Final technical report: U.S. Department of Energy; 2012, Award no: DE-EE0003638.
- [28] U.S. Energy Information Administration [Internet], Washington DC, USA. Monthly energy review. Available from: (http://www.eia.gov/totalenergy/data/monthly/pdf/sec7_5.pdf) [cited 2014 January 22].
- [29] Leaman KD, Molinari RL, Vertes PS. Structure and variability of the Florida current at 27°N: April 1982–July 1984. *J Phys Oceanogr* 1987;17(5):565–83.
- [30] Schott F, Zantopp R. Florida Current: Seasonal and interannual variability. *Science* 1985;227:308–11.
- [31] Niiler PP, Richardson WS. Seasonable variability of the Florida current. *J Mar Res* 1973;31(3):144–67.
- [32] Schmitz WJ, Richardson WS. On the transport of the Florida current. *Deep Sea Res* 1968;15:679–93.
- [33] Beal LM, Hummon JM, Williams E, Brown OB, Baringer W, Kearns EJ. Five years of Florida current structure and transport from the royal caribbean cruise ship explorer of the seas. *J Geophys Res* 2008;113(C6).
- [34] Meinen CS, Baringera MO, Garcia RF. Florida Current transport variability: an analysis of annual and longer-period time signals. *Deep-Sea Res I: Oceanogr Res Pap* 2010;57:835–48.